


Characterization of endogenous Kv1.3 channel isoforms in T cells

Julia Serna^{1,2} | Diego A. Peraza^{1,2} | Sara Moreno-Estar^{1,2} | Juan J. Saez³ |
Dino Gobelli^{2,4} | Maria Simarro^{2,4} | Claire Hivroz³ | José R. López-López^{1,2} |
Pilar Ciudad^{1,2} | Miguel A. de la Fuente^{2,4} | M. Teresa Pérez-García^{1,2} 

¹Departamento de Bioquímica y Biología Molecular y Fisiología, Universidad de Valladolid, Valladolid, Spain

²Unidad de Excelencia, Instituto de Biología y Genética Molecular (IBGM), CSIC, Valladolid, Spain

³Institut Curie, PSL Research University, INSERM U932, Integrative Analysis of T Cell Activation Team, Paris, France

⁴Departamento de Biología Celular, Genética, Histología y Farmacología, Universidad de Valladolid, Valladolid, Spain

Correspondence

M. Teresa Pérez-García, Departamento de Bioquímica y Biología Molecular y Fisiología, Universidad de Valladolid, Edificio IBGM, c/Sanz y Forés, 3, 47003 Valladolid, Spain. Email: tperez@uva.es

Funding information

Fondation pour la Recherche Médicale; Universidad de Valladolid; Ministerio de Economía y Competitividad; Junta de Castilla y León; Agence Nationale de la Recherche

Abstract

Voltage-dependent potassium channel Kv1.3 plays a key role on T-cell activation; however, lack of reliable antibodies has prevented its accurate detection under endogenous circumstances. To overcome this limitation, we created a Jurkat T-cell line with endogenous Kv1.3 channel tagged, to determine the expression, location, and changes upon activation of the native Kv1.3 channels. CRISPR-Cas9 technique was used to insert a Flag-Myc peptide at the C terminus of the *KCNA3* gene. Basal or activated channel expression was studied using western blot analysis and imaging techniques. We identified two isoforms of Kv1.3 other than the canonical channel (54 KDa) differing on their N terminus: a longer isoform (70 KDa) and a truncated isoform (43 KDa). All three isoforms were upregulated after T-cell activation. We focused on the functional characterization of the truncated isoform (short form, SF), because it has not been previously described and could be present in the available Kv1.3^{-/-} mice models. Overexpression of SF in HEK cells elicited small amplitude Kv1.3-like currents, which, contrary to canonical Kv1.3, did not induce HEK proliferation. To explore the role of endogenous SF isoform in a native system, we generated both a knockout Jurkat clone and a clone expressing only the SF isoform. Although the canonical isoform (long form) localizes mainly at the plasma membrane, SF remains intracellular, accumulating perinuclearly. Accordingly, SF Jurkat cells did not show Kv1.3 currents and exhibited depolarized resting membrane potential (V_M), decreased Ca^{2+} influx, and a reduction in the $[Ca^{2+}]_i$ increase upon stimulation. Functional characterization of these Kv1.3 channel isoforms showed their differential contribution to signaling pathways involved in formation of the immunological synapse. We conclude that alternative translation initiation generates at least three endogenous Kv1.3 channel isoforms in T cells that exhibit different functional roles. For some of these functions, Kv1.3 proteins do not need to form functional plasma membrane channels.

KEYWORDS

calcium signaling, electrophysiology, immunological synapse, Kv1.3 channels, T cells

This is an open access article under the terms of the Creative Commons Attribution-NonCommercial License, which permits use, distribution and reproduction in any medium, provided the original work is properly cited and is not used for commercial purposes.

© 2023 The Authors. *Journal of Cellular Physiology* published by Wiley Periodicals LLC.

1 | INTRODUCTION

Voltage-dependent potassium (Kv) channels comprise a large family of channels ubiquitously expressed. In excitable cells, they act as brakes for depolarization, contributing to set resting membrane potential (V_M) and dictating the duration and frequency of action potential. In nonexcitable cells, this same ability to sense and regulate V_M allows Kv channels to modulate Ca^{2+} signaling and cell volume, contributing to processes ranging from secretion to cell migration and proliferation (Pérez-García et al., 2018; Urrego et al., 2014; Wulff et al., 2009).

Kv1.3 channels were first described in T cells, where they contribute to maintain resting V_M at negative values, preventing membrane potential depolarization (DeCoursey et al., 1984). Antigen binding to T-cell receptor (TCR) is followed by a transient release of Ca^{2+} from intracellular stores, which precedes a sustained Ca^{2+} influx through Ca^{2+} release-activated Ca^{2+} (CRAC) channels that is required for complete activation (Cahalan & Chandy, 2009). The increase in $[Ca^{2+}]_i$ activates KCa3.1, a Ca^{2+} -activated and voltage-independent K^+ channel, hyperpolarizing V_M and increasing the driving force for Ca^{2+} entry.

The expression and, consequently, the functional contribution of both Kv1.3 and KCa3.1 channels varies depending on T-cell activation status (Cahalan & Chandy, 2009; Feske et al., 2015; Pérez-García et al., 2018). Kv1.3 is the predominant channel expressed both in resting T cells and in a subset of activated T cells (effector memory T cells, T_{EM}), whereas KCa3.1 is upregulated in activated naïve and central memory T cells. The differential regulation of these two channels provides interesting therapeutic applications. Kv1.3 channel blockade attenuates Ca^{2+} signaling and inhibits motility of activated T_{EM} cells in peripheral tissues, so that selective Kv1.3 blockers, either small organic molecules (e.g., 5-(4-Phenoxybutoxy)psoralen [PAP-1]) or peptides isolated from venomous animals such as ShK peptide) has been validated in different animal models for treatment of autoimmune disorders and inflammation mediated by T_{EM} cells (Beeton et al., 2006; Wulff et al., 2003).

Despite significant progress in Kv1.3 pharmacology, the use of rational drug design to create novel inhibitors and the characterization of their potential off-target effects requires the accurate characterization of Kv1.3 channels functional expression. Moreover, regardless of the ability of Kv1.3 inhibitors to impede preclinical models of autoimmune disease, it is not clear whether inhibition of Kv1.3 is sufficient to fully inhibit pathological T-cell activation and effector function, as only partial inhibition of in vitro T-cell responses has been detected using functional readouts, such as proliferation or cytokine production (Beeton et al., 2006; Schmitz et al., 2005; Wulff et al., 2003). It is known that Kv1.3 channel activity can be modulated by other factors, such as protein kinases. In addition, protein-protein interactions of Kv1.3 with other molecules determining its location and recruitment into the immunological synapse (IS) could shape Kv1.3 contribution to signal transduction in T cells (Panyi, 2005). The lack of accurate systems for detection of endogenous Kv1.3 channels is an important limitation to explore these mechanisms. To overcome these drawbacks, we aimed to develop an edited Jurkat cell line in

which endogenous Kv1.3 was tagged with different epitopes at the C terminus to facilitate its identification and location in an unambiguous way. To our surprise, the edited cell lines exhibited several isoforms of endogenous Kv1.3 channel proteins differing in their N terminus, due to the presence of at least two alternative translation initiation sites. All isoforms were upregulated upon T-cell activation. One of them was a 43 kDa Kv1.3 truncated protein (short form, SF) that can be still present in the commercially available Kv1.3 knockout (KO) mice, so we investigated its potential functional role(s). We created Jurkat cell lines expressing tagged wild type (WT) or SF channels and also a full Kv1.3-KO. We combined expression and functional studies in these cell lines with heterologous expression of the different Kv1.3 isoforms, to determine their subcellular location and their functional contribution to cell activation and proliferation. Our data indicate that these isoforms can have an impact on T-cell functions that in the case of the SF does not depend on its conductive properties at the plasma membrane.

2 | MATERIALS AND METHODS

2.1 | Cell cultures

Human T lymphocyte-derived Jurkat cell line (ATCC, TIB-152) and Human embryonic kidney HEK-293 and HEK-293FT cell lines (R70007, Invitrogen) were cultured at 37°C with 5% CO_2 in high-glucose Dulbecco's modified Eagle medium supplemented with fetal bovine serum (10%), penicillin-streptomycin (100 units/mL, sodium pyruvate (1 mM), and L-glutamine (2 mM, all from Gibco). HEK-293 cells were used for heterologous expression and the HEK-293-derived cell line 293FT was used for AAV6 generation.

Human B lymphocyte-derived Raji B cells (ATCC, CCL-86) were cultured at 37°C with 5% CO_2 in RPMI 1640 Glutamax (Gibco) with 10% fetal calf serum (FCS, Eurobio). Mononuclear cells were obtained from Etablissement Français du Sang in accordance with INSERM ethical guidelines. Cells were isolated from peripheral blood of healthy donors (both male and female donors) on a Ficoll density gradient and Human total $CD4^+$ isolation kit (Miltenyi Biotech) was used for T-cell purification. Media for primary $CD4^+$ T cells was the same as Raji B cells supplemented with 1% Penicillin/Streptomycin, 10 mM HEPES, and 0.05 mM β -mercaptoethanol (all from Gibco).

Jurkat cells were activated upon exposure for 12–16 h to different treatments, including phorbol-12-myristate-13-acetate (PMA; 100 ng/mL), Ionomycin (1 μ M), phytohemagglutinin (PHA; 2 μ g/mL), Thapsigargin (Thap, 0.2 μ M), all from Sigma. For $CD3/CD28$ crosslinked, 5 μ g/mL of mouse antihuman α CD3 was coated on 96-well plates overnight and 3×10^5 Jurkat cells were plated and stimulated with 2 μ g/mL of mouse antihuman α CD28 and 2 μ g/mL of IgG (H + L) F(ab')₂-Goat antimouse. Pro-apoptotic stimuli (Dexamethasone, 1 μ M; 2-Deoxyglucose, 10 mM; and Staurosporin, 1 μ M all from Sigma) were applied for 4 h.

For Raji B-cell-based stimulation, Raji B cells were loaded with different concentrations of Staphylococcal enterotoxin E (SEE, Toxin

Technology Inc.) for 30 min at 37°C, washed with serum-free media to remove excess toxin, and 2×10^5 Jurkat cells were mixed with 10^5 SEE-loaded Raji B cells per well in a 96-well U-bottom plate and incubated at 37°C.

2.2 | Plasmids generation

We generated several expression plasmids for KCNA3-tagged isoforms and mutants, as well as a pAAV-KCNA3-tagged plasmid to create an edited Jurkat cell line. All polymerase chain reaction (PCR) experiments were performed using Hot Start II High-Fidelity DNA Polymerase (Thermo Scientific) and purified using Wizard SV Gel and PCR Clean-Up System (Promega) following manufacturer's instructions. The protocols for the construction of all these vectors and the sequences of the primers used are detailed in the online Supporting Information.

2.3 | Cell transfection

Confluent HEK cells (70%–80%) plated on 35 mm petri dishes were transiently transfected with 1 µg of plasmid(s) DNA using Turbofect Transfection Reagent (Fisher Scientific) at a ratio DNA:Turbofect of 2:1. Kv1.x Small interfering RNAs (siRNAs) were cotransfected at a concentration of 10 nM. In all cases, the transfection mixture was left for up to 24 h. Transfection efficiency, quantified in each experiment by green fluorescent protein (GFP) or Cherry fluorescence, was always over 65%. For electrophysiological recordings, cells were then trypsinized and plated onto poly-L-lysine-coated coverslip for 24 h before use. For immunocytochemical studies and/or fluorescence microscopy, cells were seeded into poly-L-lysine-coated coverslips placed in 12 mm wells before transfection. The total amount of DNA in all cases was kept constant by adding an empty vector or a GFP vector when needed.

Jurkat cells were transfected by nucleofection using Neon Electroporation System (Thermo Fisher). Three 1700 V/20 ms pulses were applied to 10^6 Jurkat cells resuspended in 100 µL of Buffer R with 1 µg of plasmid DNA. For immunocytochemistry and/or fluorescence microscopy, cells were seeded into poly-L-lysine-coated coverslips placed in 12 mm wells after transfection.

2.4 | Jurkat T-cell knock-in generation (Kv1.3-tagged Jurkat cell lines)

Homologous recombination at the KCNA3 loci was used to generate a Jurkat cell knock-in endogenously expressing the Kv1.3 protein tagged with a 3xFLAG-2MYC peptide or a NeonGreen fluorescence protein. This strategy combines two main elements: the CRISPR-Cas9 system directed to the KCNA3 gene to create a double-strand break and an AAV6 transduction vector with the DNA donor, containing two homology arms from the KCNA3 gene flanking the exogenous

TAG sequence (3FLAG-2MYC or 3FLAG-NeonGreen) and a blasticidin resistance gene, to allow selection of edited cells. The detailed procedures can be found in the online Supporting Information.

2.5 | Jurkat T-cell KO generation

Two Jurkat KO models, a Jurkat cell line lacking LF-Kv1.3 (expressing only the SF-Kv1.3 isoform) and a total Kv1.3 KO cell line, were generated with CRISPR-Cas9 tool. Guide RNAs (gRNAs) were designed using the CRISPOR software (primers F16/R16 to F18/R18 in Supporting Information: Table I). Two gRNAs located at the beginning and at the end of the KCNA3 were selected to eliminate the complete exon (total KO), whereas the SF-Kv1.3-expressing clone was generated by choosing two gRNAs located both at the 5'-end of the KCNA3 gene. All gRNAs were generated using GeneArt Precision Synthesis Kit.

3FLAG-2MYC (10^6) homozygous-tagged Jurkat cells were Nucleofected with 5 µg of Cas9 and 500 ng of each gRNA, and a limiting dilution was performed to establish individual clones, which were confirmed by western blot analysis.

2.6 | Protein determinations

Western blotting protocols were performed as described elsewhere (Cidad et al., 2020). Briefly, 10^6 cells were lysed in 50 µL of radioimmunoprecipitation assay buffer (20 mM Tris pH 7.4, 150 mM NaCl, 1 mM EDTA, 0.1% sodium dodecyl sulfate [SDS], 1% sodium deoxycolate, 1% Nonidet P-40, protease inhibitor cocktail [Sigma-Aldrich]). 50 µg of protein lysates were loaded into 10% SDS-polyacrylamide gel electrophoresis, transferred into a polyvinylidene difluoride membrane and blocked with 5% milk plus 5% bovine serum albumin (BSA) TTBS (Tween-Tris Buffered Saline) for 1 h. Primary and secondary antibodies used are listed in Table 2 (Supporting Information). Images were acquired with a VersaDoc 4000 Image System (Bio-Rad) and quantified using ImageJ software.

For western blot analysis of phosphorylated proteins, a flat-bottom 96-well plate was coated with 10 µg/mL of mouse antihuman CD3 and 10 µg/mL of mouse antihuman CD28 overnight. To activate the cells, 3×10^5 Jurkat T cells per well were seeded and incubated at 37°C for 10 min. The activation was stopped by directly adding 10× lysis buffer and incubating the plate for 15 min on ice. Postnuclear lysates obtained by centrifugation at maximum speed for 10 min at 4°C and were kept at -20°C until immunoblot analysis.

For immunocytochemistry, cells seeded into poly-L-lysine-coated coverslips were fixed with 4% paraformaldehyde and blocked in phosphate-buffered saline (PBS) with 2% BSA using a permeabilizing blocking solution. Cells were incubated overnight at 4°C with primary antibody (anti-Flag M2, 1:200, Sigma), followed by PBS washes and 1 h incubation with 1:1000 goat antimouse 532 secondary antibody (Molecular Probes). After labeling nuclei (Hoechst 33342; 1:2000), coverslips were mounted with Vectashield (Vector Laboratories).

Photomicrographs were acquired with a LEICA SP5 confocal microscope using LAS software. In the case of HEK cells transfected with Cherry or GFP fusion proteins, Hoechst was added after fixing the cells.

2.7 | Electrophysiological methods

Ionic currents were recorded at room temperature using cell-attached, whole-cell, or perforated-patch configurations of the patch clamp techniques as previously described (Jiménez-Pérez et al., 2015; Ciudad et al., 2020). Details of the protocols and the solutions used can be found in the online Supporting Information.

2.8 | Intracellular calcium determination

For intracellular calcium measurements, Jurkat cells were seeded on poly-L-lysine-treated glass coverslips and after 24 h cells were loaded with 2 μ M of the fluorescent Ca^{2+} indicator Fluo-4-AM (Molecular Probes, Invitrogen) for 1 h at room temperature. Then cells were placed on the stage of an inverted microscope, treated with 200 nM Thapsigargin, and bathed in a 0 mM Cl_2Ca tyrode solution to deplete intracellular Ca^{2+} . After that, intracellular Ca^{2+} changes in response to application of 2 mM Cl_2Ca tyrode solutions were explored. At the end of the experiment, cells were exposed to 10 μ M of the protonophore CCCP (Carbonyl cyanide 3-chlorophenylhydrazone) plus 5 μ M of Ca^{2+} ionophore ionomycin to determine f_{max} . Intracellular calcium images were acquired using an inverted microscope, Eclipse TE (Nikon), equipped with a Nikon CFI S Fluor ($\times 40$, numerical aperture = 1.30) oil-immersion objective and a Sensi Cam (PCO AG) camera. Images were acquired with Imaging Workbench 4.0 software. Background-subtracted fluorescence signals were expressed as $f/(f_{\text{max}} - f)$.

2.9 | Proliferation studies

The percentage of HEK cells at the S phase was quantified using 5-ethynyl-2'-deoxyuridine (EdU) incorporation as previously described (Ciudad et al., 2020). HEK cells transfected with WT-Kv1.3, LF-Kv1.3, or SF-Kv1.3, as GFP fusion proteins were trypsinized and seeded at a density of 50,000 cells/well on 12 mm poly-lysine-coated coverslips. Twenty-four hours after seeding, EdU was added for 20 min and proliferation was measured with Click-iT[®] EdU Imaging Cell Proliferation Assay (Invitrogen). Determinations were carried out in triplicate samples and controls were included in all experiments.

2.10 | T-cell cytokine secretion assay

We determine interleukin-2 (IL-2) secretion in Jurkat cells in response to cell activation with CD3/CD28, PMA + PHA-P, and

Raji B-cell-based stimulation. Secretion of IL-2 and tumor necrosis factor- α (TNF- α) was also determined on CD4⁺ human T cells stimulated with 1:1 CD3/CD28-coated Dynabeads (Thermo Fisher Scientific) for 16 h at 37°C. Then, cytokines concentration was quantified from supernatants by enzyme-linked immunosorbent assay (Peprotech) according to manufacturer's instructions. In experiments analyzing the effect of the Kv1.3 inhibitors PAP-1 (100 nM) and Margatoxin (MgTx; 10 nM), cells were pretreated with the blockers 1 h before stimulation. All experiments were performed in technical duplicates and biological triplicates.

2.11 | ISs studies

Raji B cells (1×10^6 cells/mL) were labeled with CellTracker Blue CMAC dye (10 μ M, Thermo Fisher) in RPMI without FCS for 20 min at 37°C and incubated with 100 ng/mL SEE for 30 min at 37°C (Saez et al., 2021). SEE-loaded Raji cells and Jurkat cells were cocultured on coverslips for 30 min at 37°C at a ratio 1:1, were washed with PBS, fixed with 4% paraformaldehyde, quenched with 10 mM glycine for 10 min, and permeabilized with staining buffer (PBS + 0.2% BSA + 0.05% saponin) for 30 min. After 1 h incubation with human anti-GFP (Recombinant Antibody Platform, Institut Curie) and rabbit anti-pLAT primary antibody (Cell Signaling), cells were washed with staining buffer and incubated for 30 min with 1:500 anti-Human Alexa-488, anti-rabbit Alexa-568 secondary antibodies (Invitrogen, Thermo Fisher), and phalloidin-647 (Invitrogen, Thermo Fisher). Coverslips were mounted with Fluoromount G (SouthernBiotech). Images were acquired using an inverted laser scanning confocal microscope (Leica DMI8, SP8 scanning head unit), equipped with HC PL APO CS2 $\times 63/1.40$ oil objective. ImageJ software and compatible scripts were generated for automated or semiautomated analysis.

2.12 | Statistical analysis

Statistical analysis was performed using R software packages. Pooled data from several different experiments are expressed as mean values \pm SEM. Shapiro-Wilk test and Bartlett's test were used to test normality and homogeneity of variances, respectively. For comparisons among several groups, one-way analysis of variance followed by Tukey's test was employed in the case of normal distributions and equal variances; alternatively, Kruskal-Wallis analysis followed by Dunn's test was applied. Differences were considered statistically significant when $p < 0.05$.

3 | RESULTS

3.1 | Generation of a Kv1.3-tagged Jurkat cell line

CRISPR-Cas9 tool was used to generate edited Jurkat cells with a tag peptide in Kv1.3 endogenous channels before the STOP codon.

Jurkat clones with fusion proteins of Kv1.3 with the fluorescent protein mNeonGreen or with 3Flag2Myc peptide were obtained. Basal Kv1.3-NeonGreen Jurkat cell line fluorescence was weak on unstimulated cells, but easily detected in live cells upon PMA + ionomycin activation, which induces a strong upregulation of Kv1.3 channels (Panyi et al., 2004) confirmed by whole-cell recordings of voltage-dependent K⁺ currents (Kv) in Jurkat cells at rest and after activation. These Kv currents were fully abolished by the selective Kv1.3 blocker PAP-1, as shown for the rest condition in the representative current traces (Figure 1a).

Kv1.3-3Flag2Myc Jurkat cell lines were used to study endogenous Kv1.3 channel regulation. Using anti-Flag antibody to detect the expression of Kv1.3 in edited Jurkat clones after immunoprecipitation, we observed a band of the expected size (around 66 KDa with the tag sequence) and two additional bands of around 43 and 85 KDa (Figure 1b). The same band pattern could be observed

in HEK cells overexpressing the tagged Kv1.3-3Flag2Myc construct (Figure 1c). In edited Jurkat cells, expression of all bands was upregulated after stimulation with different activating (but not with proapoptotic) signals (Figure 1d). The changes in expression among the three bands were similar in all cases, regardless of the intensity of the activation.

3.2 | Endogenous Kv1.3 channels show different isoforms

To determine if these bands reflect different Kv1.3 channel isoforms, and considering that Kv1.3 is a single exon gene, a bioinformatics search of translation initiation sites in the *KCNA3* messenger RNA (mRNA) sequence was performed. We identified four start codons that could be the origin of the proteins observed by western blot

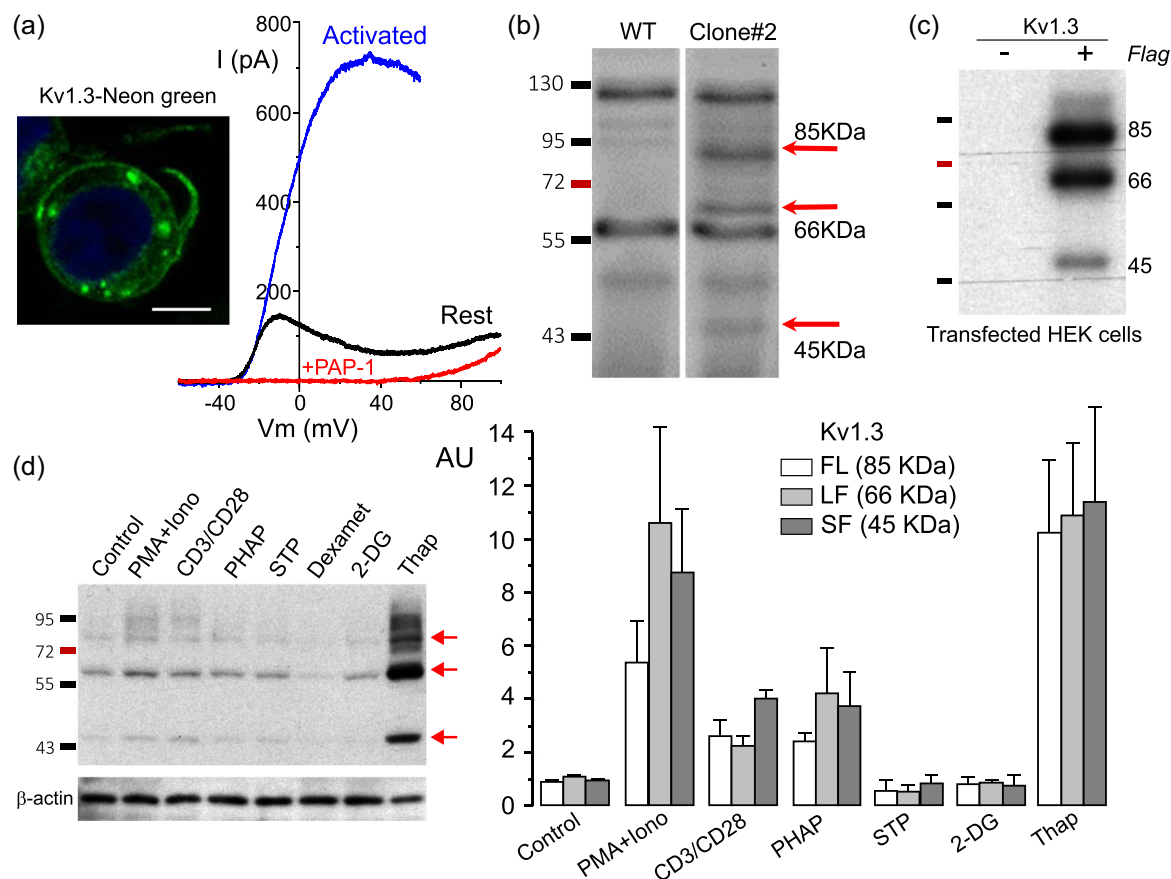


FIGURE 1 Characterization of Kv1.3-tagged Jurkat cell lines. (a) Confocal image obtained in live Jurkat-NeonGreen cells stimulated for 16 h with phorbol-12-myristate-13-acetate (PMA) + ionomycin. Representative 2 s voltage ramps from -80 to +10 mV obtained in an edited cell before (black) and after applying 100 nM 5-(4-Phenoxybutoxy)psoralen (PAP-1) (red). The blue trace is a representative ramp obtained in an edited cell previously activated with PMA + ionomycin. Scale bar = 5 μ m. (b) Kv1.3-3Flag-2Myc Jurkat cells immunoprecipitated and immunoblotted with anti-Flag antibody showed three bands of the indicated sizes (red arrows). (c) Western blot analysis obtained with the anti-Flag antibody from lysates of HEK cells transfected with untagged-Kv1.3 plasmid (-) or Kv1.3-3Flag plasmid (+), showing the same three bands observed in (b). (d) Representative immunoblot obtained with the anti-Flag antibody from total Kv1.3-3Flag-2Myc Jurkat cell lysates at rest (left lane) or after incubation with the indicated activating or proapoptotic stimuli. The bar plot shows the protein quantification of the 85 KDa (FL), 66 KDa (long form [LF]), and 43 KDa (short form [SF]) after normalization with β -actin in arbitrary units. Each bar is the mean \pm SEM of three to five independent experiments.

(Figure 2a). To confirm that, we transfected HEK cells with plasmids containing the *KCNA3* gene with mutations to alanine of each putative starting methionine (Figure 2b). Mutation of the first methionine, (Met1, M0 in Figure 2a) abolished translation of the 85 KDa band. Mutation of the second methionine (Met53, M1) eliminated the canonical 66 KDa band. No changes were observed when mutating the third methionine (Met137), indicating that it was not a translation initiation site. Finally, mutation of the fourth methionine (Met194, M2) eliminated the 43 KDa band. These results demonstrate that there are at least three translation initiation sites in the *KCNA3* coding region.

We also created plasmids expressing either the canonical Kv1.3 protein alone (the long form [LF] carrying a mutation to alanine of the M2 methionine) or the short 43 KDa isoform (SF) as GFP or mCherry fusion proteins (Figure 2c,d) to explore the expression and function of these isoforms. When expressed in HEK cells, we observed that LF

expression was restricted to the plasma membrane, whereas SF seemed almost exclusively intracellular, delimitating the nuclear membrane and the endoplasmic reticulum. There was almost no colocalization between both Kv1.3 isoforms (see merged LF + SF image in Figure 2c). The lack of membrane expression of the SF could also be demonstrated by cotransfection with another channel with predominant expression at the plasma membrane, as it is the case of the Orai channel (Figure 2d). Finally, and contrary to previous reports describing mitochondrial Kv1.3 channels (Szabò et al. 2005, 2008), live-cell confocal images of WT Kv1.3 channels coexpressed with MitoTracker did not show colocalization (Figure 2e), live-cell confocal images of WT Kv1.3 channels coexpressed with MitoTracker did not show colocalization (Figure 2e). This result was confirmed in fixed cells cotransfected with SF and the mitochondrial-targeting signal (MTS) of the cytochrome c oxidase subunit 8A (COXa) fused to a mCherry protein as a mitochondria marker (mitoCherry, Figure 2f). Although these data do not rule out the expression of some Kv1.3 channels at the mitochondria, they indicate that these

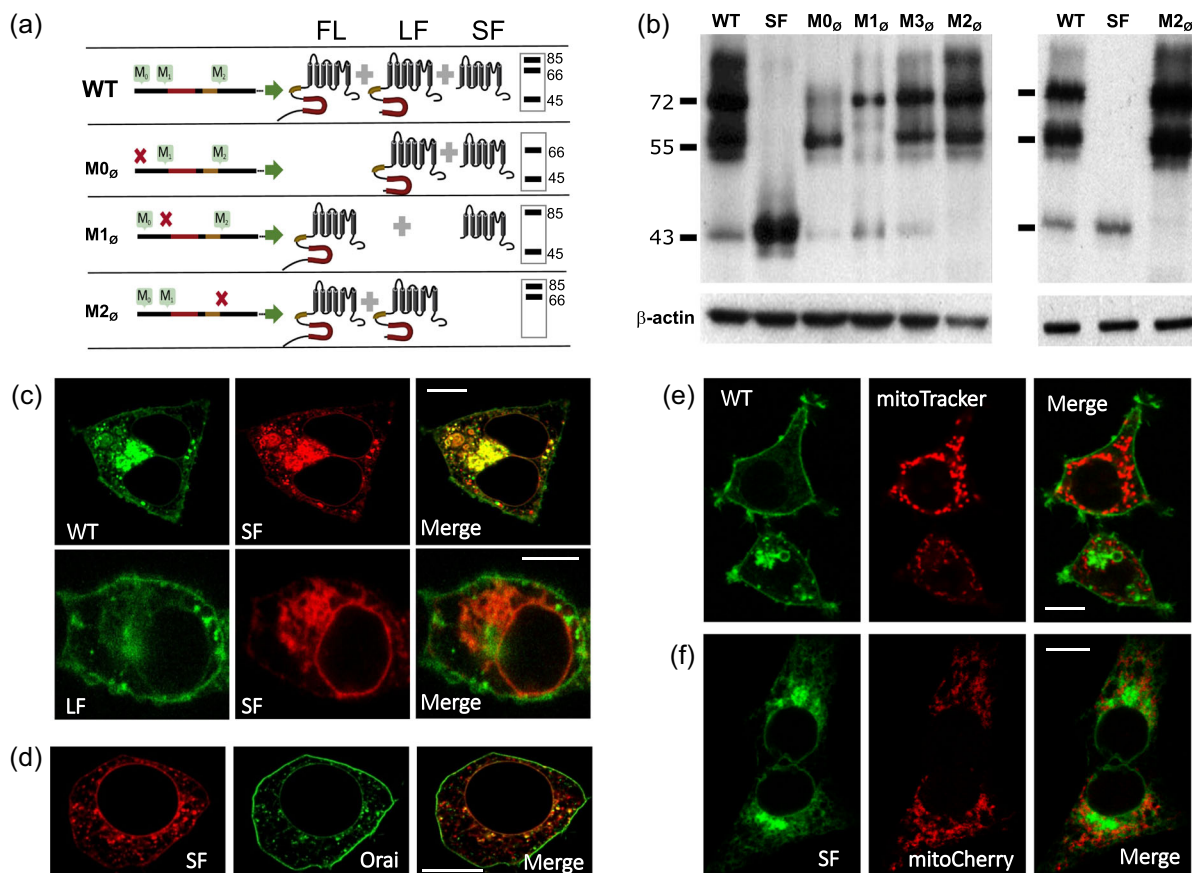


FIGURE 2 Endogenous Kv1.3 channel isoforms. (a) Schematic representation of the position of the Kv1.3 Methionines M0, M1, and M2, and the expected outcome of their individual mutation to alanine (M0_ø, M1_ø, M2_ø, see text for more details) in a Kv1.3-3Flag plasmid.

(b) Representative immunoblots obtained with anti-Flag antibody on HEK cells lysates transfected with wild type (WT) Kv1.3-3Flag plasmid (WT), SF-Kv1.3-3Flag plasmid encoding the 43 KDa protein (short form [SF]) or the different point mutants M0–M3. M0–M2 mutants showed the band pattern depicted in the scheme of part A, whereas M3_ø mutant (Met137) was not different from WT and is not shown in the scheme. (c, d) Confocal images obtained in HEK cells transfected with WT Kv1.3-eGFP (WT), the SF of Kv1.3 fused with Cherry (SF), the long form (LF) fused with enhanced green fluorescent protein (eGFP) (LF), or the Orai-1 channel fused with eGFP (Orai). The panels show the green and red fluorescence, and merged images. (e) Live-cell confocal images of HEK cells expressing WT Kv1.3-eGFP and mitoTracker probe. (f) Confocal images obtained in fixed HEK cells cotransfected with SF-eGFP and mitoCherry plasmids. No colocalization was observed in the merge panels in (e) and (f). (c–f) Scale bars = 10 µm.

organelles do not represent a preferential location for any Kv1.3 channel isoform.

However, we identified a Methionine (Met357) in the Kv1.3 sequence before a consensus MTS (HEIJNE et al., 1989). MTS shows a high degree of similarity to the S4 transmembrane α -helix of Kv channels (Supporting Information: Figure 1A). We created an additional construct with this truncated Kv1.3 channel (mito-Kv1.3) as GFP fusion protein. Mito-Kv1.3 construct encoded a 25–30 KDa band that could not be detected in endogenous or overexpressed Kv1.3 channels (Supporting Information: Figure 1B), suggesting that Met357 does not represent a Kv1.3 alternative translation initiation site. Still, we investigate whether this mito-Kv1.3 could be directed to mitochondria upon overexpression in HEK cells. Cotransfection with mito-Cherry (MTS-COX8A) showed a complete lack of colocalization, indicating that even if this mito-Kv1.3 isoform were expressed it could not be located at the mitochondria. To our surprise, in the absence of the Kv1.3 fragment this Kv1.3 MTS sequence was able to send GFP to the mitochondria (Supporting Information: Figure 1C), suggesting that even though Kv1.3 MTS sequence does behave as a MTS, mito-Kv1.3 protein is not expressed under native conditions.

3.3 | Functional characterization of Kv1.3 channel isoforms in HEK cells

To confirm expression (and location) data, functional characterization of these two isoforms, together with the WT Kv1.3 channels, was carried out with electrophysiological studies in transfected HEK cells (Figure 3). We explored the current density in depolarizing pulses to +40 mV (a), the steady-state inactivation (b), the use-dependent block upon high-frequency pulses (c), and the sensitivity to block with the selective blocker PAP-1 (d). LF overexpression elicited large voltage-dependent Kv1.3 currents with kinetic and pharmacological properties indistinguishable from WT currents. SF constructs elicited significantly smaller Kv1.3 currents with a leftward-shift of the midpoint of inactivation. These results, together with the scarce membrane location of the SF isoform suggest that SF alone does not form conducting channels. The small currents observed could be mediated by heteromultimers with endogenous HEK cells Kv1.x channels. In support of this hypothesis, we found that when HEK cells were cotransfected with SF and a mixture of siRNAs against Kv1.1 and Kv1.6 channels (the most abundant endogenous Kv1 channels in our HEK cells), there was a

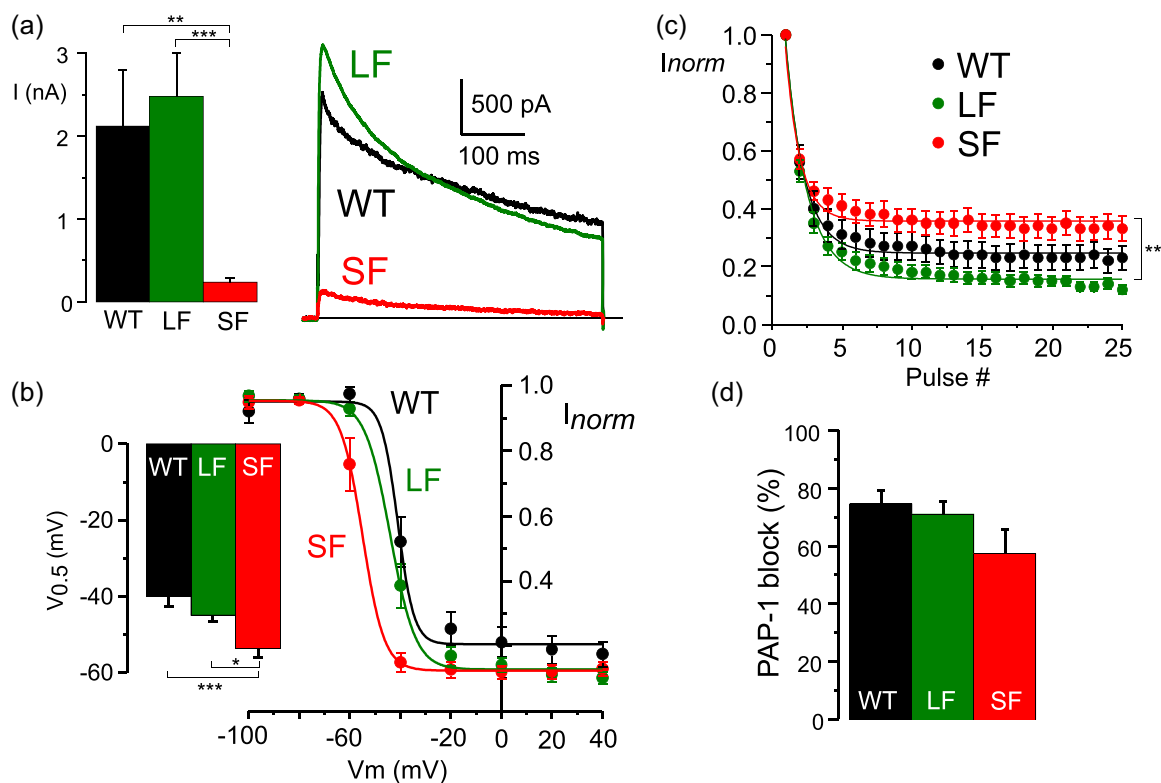


FIGURE 3 Functional characterization of Kv1.3 channel isoforms in HEK cells. (a) Average current amplitudes were obtained from HEK cells transfected with wild type (WT), long form (LF), or short form (SF) plasmids by measuring the peak current amplitude in 450 ms depolarizing pulses to +40 mV from a holding potential of -80 mV in cell-attached configuration. Representative traces in each condition are shown in the inset. (b) Steady-state inactivation curves were obtained with a two-pulse protocol (Cidad et al., 2020) by plotting the amplitude of a +40 mV pulse as a function of the prepulse voltage. Normalized currents are represented. The inset shows the mean \pm SEM of the midpoint of steady-state inactivation ($V_{0.5}$) obtained from the individual Boltzmann fit of each cell. (c) Use-dependent block analysis of WT, LF, and SF was carried out by the fit to an exponential decay of normalized peak current amplitudes obtained from trains of pulses to +40 mV at 0.5 Hz. (d) The sensitivity to 5-(4-Phenoxybutoxy)psoralen (PAP-1) was explored in depolarizing pulses to +40 and expressed as the % of current block upon application of 200 nM PAP-1 in the external solution. All through this figure, data are mean \pm SEM of 12–16 cells from at least three independent experiments. * $p < 0.05$; ** $p < 0.01$; *** $p < 0.001$.

significant reduction of the total current density without changes in the kinetics of the currents (Supporting Information: Figure II).

3.4 | Functional characterization of SF-Kv1.3 channels in Jurkat cells

The study of the expression and function of the SF isoform poses a relevant issue, as the mRNA codifying for this truncated protein may be present in the commercially available Kv1.3 KO mice (Koni et al., 2003). This extent was confirmed in our laboratory by PCR of samples obtained from macrophages of Kv1.3 KO (Figure 4a). To explore this isoform under endogenous conditions, we generated Kv1.3-KO Jurkat clones (eliminating the full *KCNA3* gene) and SF Jurkat clones, expressing only the SF isoform which could represent the case of the Kv1.3 KO mice (Figure 4b). Both SF and KO clones were created from the Kv1.3-3Flag2Myc Jurkat line.

Immunocytochemistry using α -Myc antibody showed a very different distribution of WT channels (with a clear plasma membrane expression) and SF proteins (Figure 4c). Accordingly, whole cell recordings did not show any Kv current in resting conditions or after 16 h activation with PMA + Ionomycin in SF or KO clones. Meanwhile, WT edited clones exhibited Kv currents significantly upregulated upon activation (Figure 4d).

The absence of functional Kv currents in the plasma membrane of SF and KO clones was further confirmed with current-clamp experiments with the perforated-patch technique (Figure 5a), which showed depolarizing resting V_M in both cases. Resting V_M in the WT clones was significantly different as it was the amplitude of the response to a depolarizing stimulus (an external solution with 60 mM K^+), although the values of V_M in the presence of 60 mM K^+ were not significantly different in all three conditions.

Hyperpolarized resting V_M of T cells due to Kv1.3 channels expression has been described to play an important role regulating

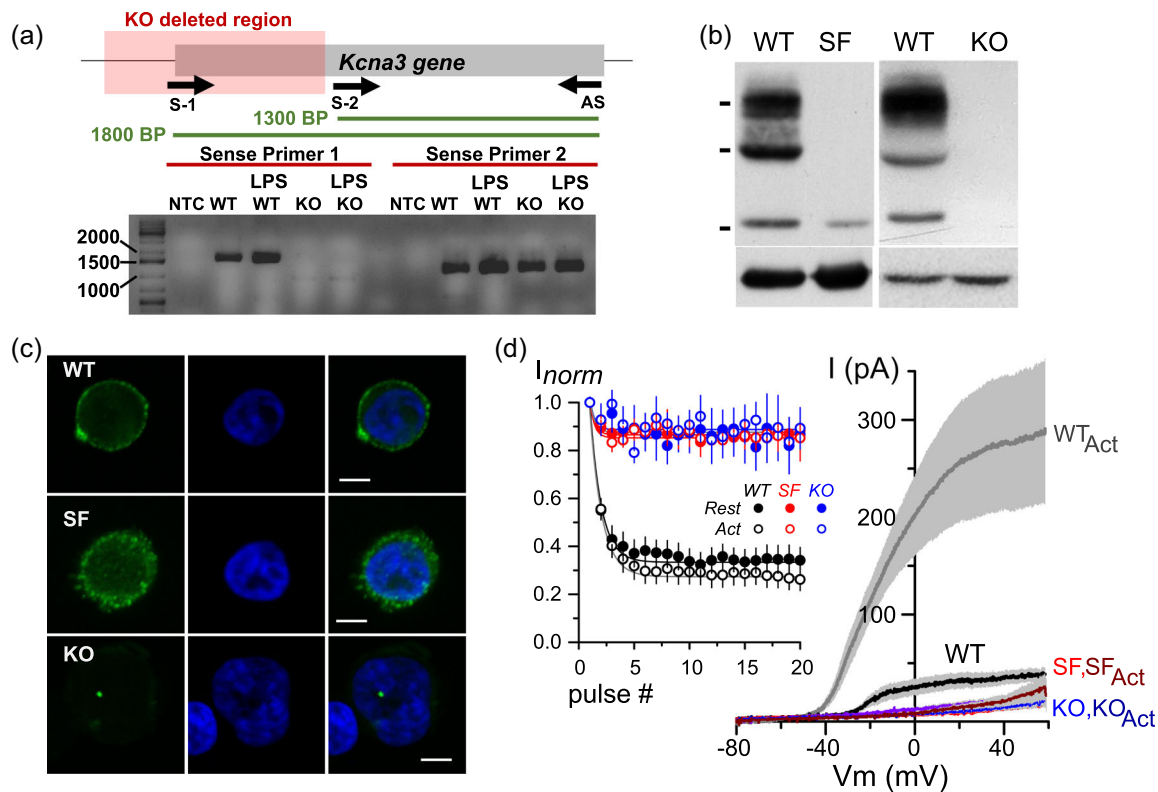


FIGURE 4 Functional characterization of SF-Kv1.3 channels in Jurkat cells. (a) Gel electrophoresis of polymerase chain reaction (PCR) products obtained with primers annealing in the 5'-region of the *kcnj3* gene (absent in the Kv1.3 knockout [KO] mouse, S-1) or in the 3'-region of the *kcnj3* gene (conserved in the Kv1.3 KO, S-2) and the same antisense primer (AS). PCR was performed of complementary DNA (cDNA) obtained from total RNA extracted from wild type (WT) and KO Kv1.3 mouse bone marrow-derived macrophages at rest and after 6 h stimulation with 100 ng/mL of lipopolysaccharide (LPS) to induce Kv1.3 expression. NTC, no template control. (b) Representative immunoblot of cell lysates from tagged Jurkat Kv1.3-3Flag-2Myc (WT), SF-3Flag-2Myc (SF), or KO clones with anti-Flag antibody. (c) Confocal images obtained in tagged WT, short form (SF), and KO Jurkat clones stained with anti-Myc antibody labeled with green fluorescent protein (GFP). The panels show GFP fluorescence (green), nuclear staining (Hoechst, blue), and the merged images. Scale bar = 5 μ m. (d) Kv currents were elicited by 2 s voltage ramps from -80 to $+60$ mV in WT, SF, and KO edited Jurkat cells at rest or activated (Act) by 16 h treatment with phorbol-12-myristate-13-acetate (PMA) + Ionomycin. The inset shows the use-dependent block analysis from a train of depolarizing pulses to $+40$ mV. The peak amplitude (normalized to pulse #1) is plotted as a function of the pulse number in each experimental condition. Data are mean \pm SEM of 18–26 cells in each condition. Cells were obtained from at least 4 different experiments and two independent Jurkat clones.

Ca²⁺ entry (Lin et al., 1993), so we studied whether [Ca²⁺]_i or the kinetics of Ca²⁺ influx were affected in edited cells. Microfluorometric studies were carried out in Jurkat cells incubated with Fluo4. After 10 min in a nominally Ca²⁺ free external solution with 200 nM Thap, reintroduction of Ca²⁺ in the external solution led to an increase in the [Ca²⁺]_i that showed a larger magnitude and a faster kinetics in the WT Jurkat clones (Figure 5b), as expected if the driving force for Ca²⁺ entry is dependent of resting V_M as described. Again, no significant differences regarding the amplitude and kinetics of Ca²⁺ fluxes were observed between SF and KO clones.

3.5 | Contribution of Kv1.3 channels isoforms to Jurkat cell function

Next, we explore whether these differences at the single-cell level translate into functional T-cell responses and whether the SF-Kv1.3 protein may have a functional impact in T-cell function despite not being able of forming a plasma membrane Kv channel. We studied some integrated functional readouts such as proliferation (for HEK cells) or cytokine secretion (in the case of Jurkat cells). As previously

described (Cidad et al., 2010), Kv1.3 overexpression increased HEK cell proliferation (Figure 6a). This effect was reproduced with LF overexpression, whereas SF overexpression had no effect.

In Jurkat cells, the levels of IL-2 in cell supernatants increased after treatment with PMA + PHA-P, polyclonal activation with anti-CD23/CD28, or exposure to Raji B cells loaded with two different SEE concentrations (Figure 6b). However, no differences in the response of the WT, SF, or KO clones were observed. In fact, contrary to previous publications (Beeton et al., 2006; Zhao et al., 2013), IL-2 secretion response was insensitive to selective Kv1.3 blockers such as PAP-1 or MgTx, both in Jurkat clones or in native T cells (Figure 6c,d). In these later ones, the secretion of another cytokine, TNF-α, was also unaffected by Kv1.3 blockers. Altogether, our data indicate that Kv1.3 channels do not take part in stimulus-induced cytokine secretion in these preparations.

3.6 | Contribution of Kv1.3 channels isoforms to Jurkat activation and IS formation

These results prompted us to explore the role of Kv1.3 channel isoforms in other T-cell responses, by analyzing their contribution in

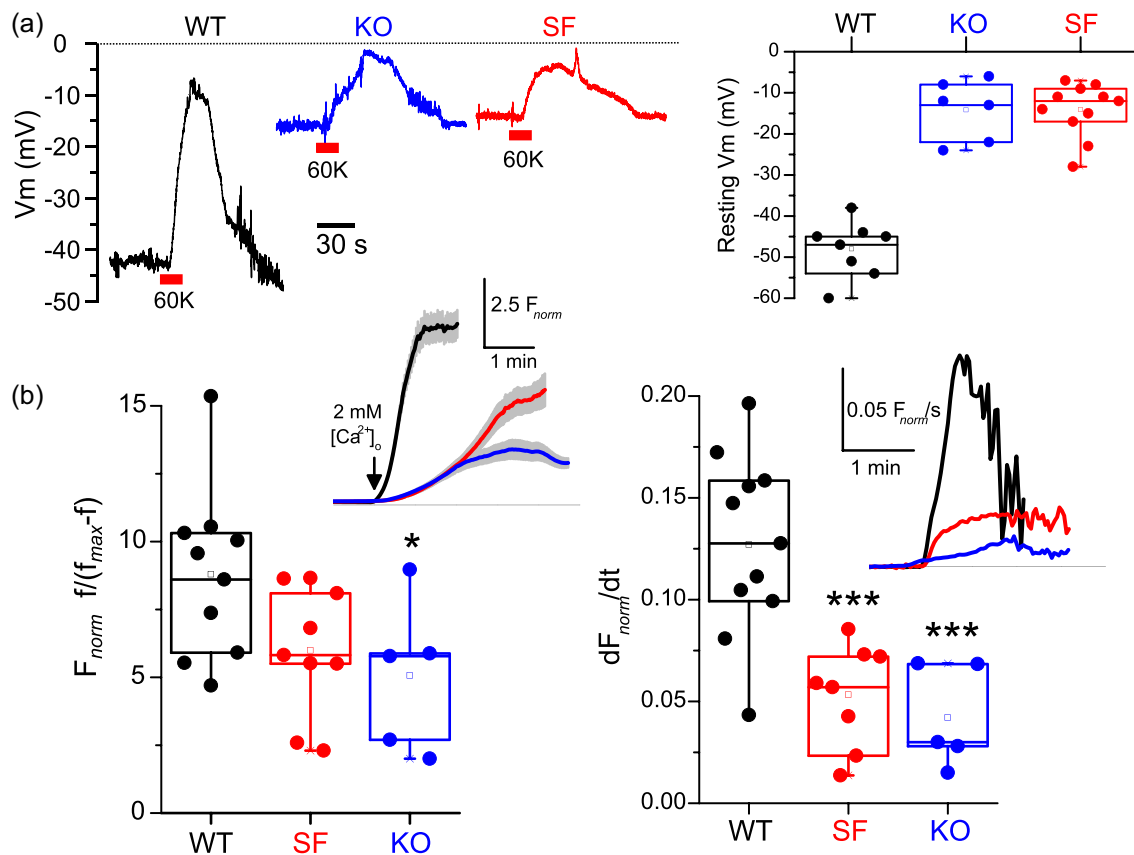


FIGURE 5 Contribution of Kv1.3 channel isoforms to resting V_M and Ca²⁺ influx. (a) Representative traces of the resting V_M recordings in wild type (WT), short form (SF), and knockout (KO) Jurkat cells with the current-clamp configuration, and the response to application of a 60 mM K⁺ external solution. The box plot shows the average resting V_M data in the three groups. (b) Box plots showing Fluo4-normalized fluorescence (as an indicator of [Ca²⁺]_i) and the derivative of the fluorescence (dF/dt), as an indicator of the kinetics of Ca²⁺ influx upon perfusion with a 2 mM Ca²⁺ solution. Each dot is the average of 30–50 cells from an independent experiment and the insets show the mean ± SEM of all cells in one of these individual experiments in WT, SF, and KO as indicated. **p* < 0.05; ****p* < 0.001 versus WT.

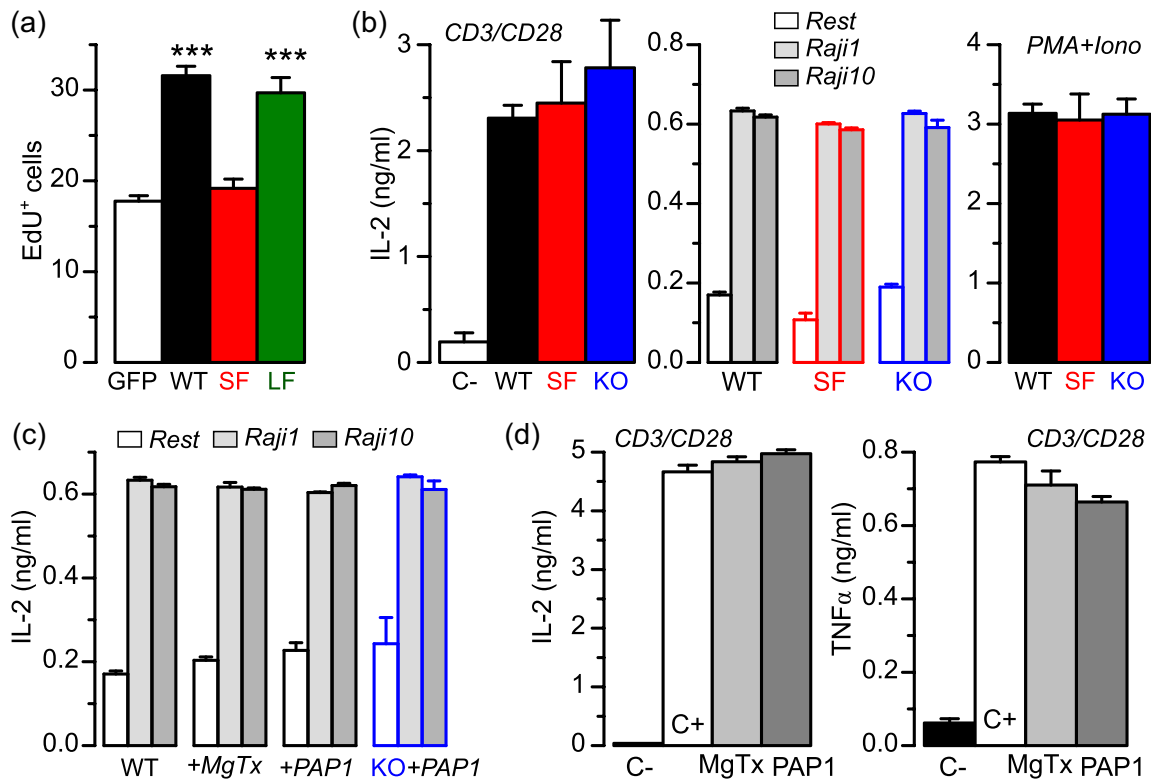


FIGURE 6 Role of Kv1.3 channel isoforms in proliferation and cytokine secretion. (a) The proliferation rate of HEK cells transfected with the indicated plasmids was determined as a percentage of the proliferation observed in control conditions (green fluorescent protein [GFP]-transfected HEK cells) using 5-ethynyl-2'-deoxyuridine (EdU) incorporation. Each bar is mean \pm SEM, $n = 6$ –15 data from 3 to 6 different experiments (** $p < 0.001$ vs. GFP). (b) The levels of interleukin-2 (IL-2) were quantified by enzyme-linked immunosorbent assay (ELISA) in supernatants from wild type (WT), short form (SF), and knockout (KO) Jurkat cell clones at rest or after 12–16 h of stimulation with anti-CD23/CD28, phorbol-12-myristate-13-acetate (PMA) + phytohemagglutinin (PHA) or exposure to Raji B cells loaded with 1 ng/mL or 10 ng/mL of Staphylococcal enterotoxin E (SEE). (c) IL-2 secretion in response to Raji B-cell stimulation was measured in WT or KO Jurkat cells preincubated for 30 min with Kv1.3 inhibitors 5-(4-Phenoxybutoxy)psoralen (PAP-1) (100 nM) or Margatoxin (MgTx, 2 nM). (d) IL-2 and tumor necrosis factor- α (TNF- α) secretion were also quantified with ELISA in human-derived CD4+ T cells. Cells were preincubated with PAP-1 or MgTx before stimulation with CD3/CD28 for 16 h. Each bar (b–d) is mean \pm SEM of at least three independent experiments.

the early steps after stimulation. We studied the phosphorylation of proteins implicated in TCR-induced signaling cascade such as phosphorylation of the CD3 ζ chain, of the zeta-chain-associated protein kinase 70 (ZAP-70 kinase), or of the linker for activation of T cells (LAT), as well as other signaling complexes further downstream in the signaling cascade such as phospholipase C γ (PLC γ) or extracellular signal-regulated kinase (ERK).

Phosphorylation of ERK in response to CD3/CD28 stimulation was reduced in KO Jurkat clones compared with WT or SF clones (Figure 7a), suggesting a functional role for both the full-length and the truncated protein in Jurkat cell activation. The characterization of phosphorylation of other proteins involved in the activation pathway showed three different patterns (Figure 7b) as follows: (i) Some (such as CD3 or ZAP-70) were independent of Kv1.3 protein and hence unaffected by the truncated isoform or the complete KO of the channel; (ii) some others required either the WT or the SF (as pERK), being significantly reduced only in KO clones. This was the case for PLC and LAT phosphorylation; and (iii) full activation of one of them, SLP76, was only achieved in WT clones, being significantly reduced in both SF and KO cells.

Both cytosolic SLP76 and membrane-associated LAT are key adaptor proteins phosphorylated by TCR-associated ZAP70, forming microclusters at the IS. Phosphorylation of LAT recruits SLP76 to the cell membrane, where they nucleate a multimolecular complex, which induces a host of downstream responses, including calcium influx, ERK phosphorylation, integrin activation, and cytoskeletal reorganization. We speculated that decreased activation of these adaptors, by affecting their translocation and/or interaction with the proteins of the signaling complexes, will impact IS formation.

We explored the degree of Kv1.3 colocalization at the IS overexpressing GFP-labeled WT, LF, or SF isoforms in Jurkat cells before Raji cell exposure. Confocal microscopy images (Figure 8a) showed a restricted plasma membrane location for LF, with a distribution close to the cortical filamentous actin, and at the IS area (labeled with pLAT). In contrast, GFP fluorescence of SF-transfected Jurkat cell was excluded from actin and pLAT-labeled regions at the IS, being restricted to a perinuclear location. A combination of both patterns was observed, as expected, in the case of the WT Kv1.3 overexpression.

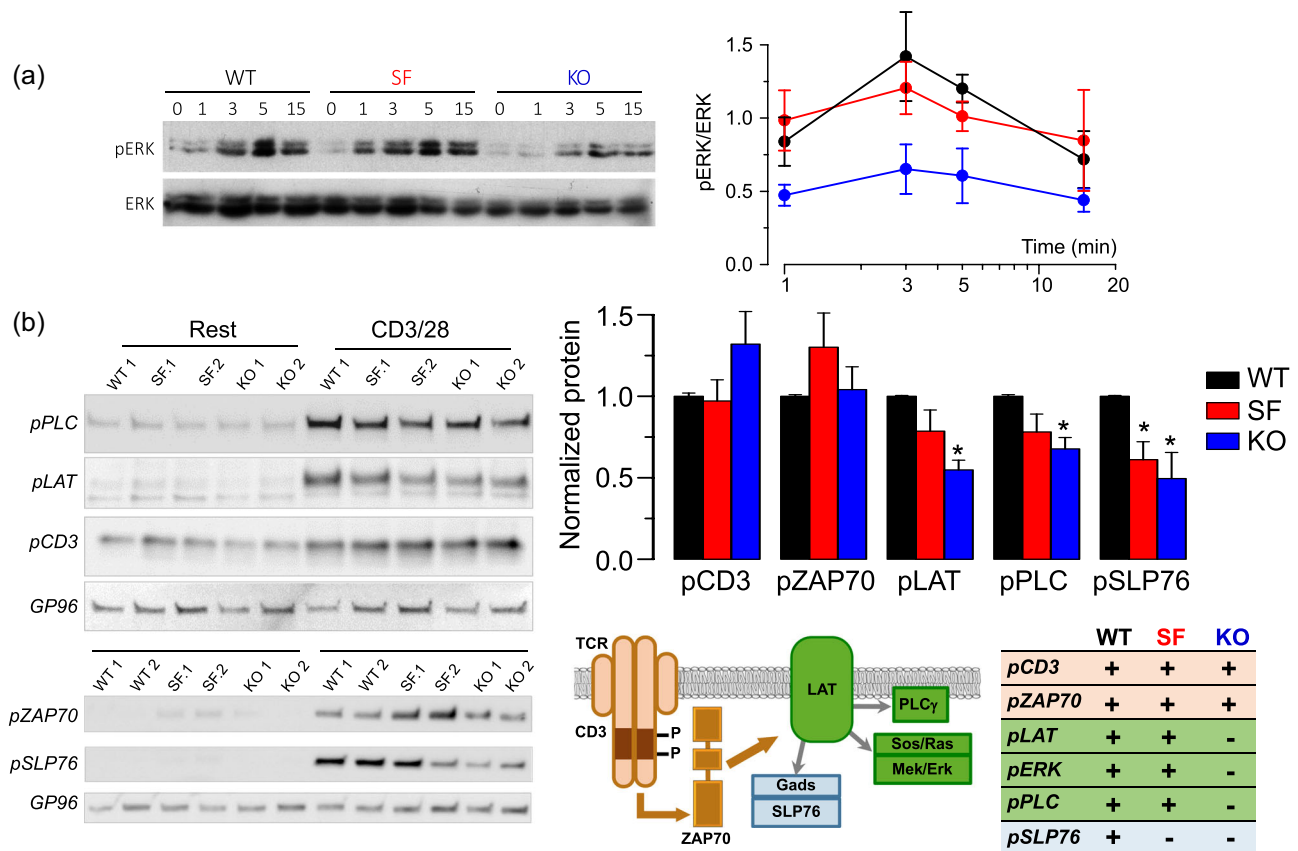


FIGURE 7 Contribution of Kv1.3 channel isoforms to T-cell signaling pathways. (a) Representative immunoblot of total Erk and pErk protein obtained from wild type (WT), short form (SF), and knockout (KO) Jurkat cell lysates incubated in the presence of soluble CD3/CD28 + secondary crosslink antibody for the indicated time intervals. Erk phosphorylation was normalized to total Erk amount. The plot shows mean ± SEM, $n = 3$. (b) Representative immunoblots of the indicated proteins determined from Jurkat cell lysates (WT, SF, and KO) at rest and after incubation in the presence of plate-fixed CD3/CD28 for 10 min. Quantification was performed using ImageJ and the amount of protein normalized for GP96 is represented in the bar graph. Mean ± SEM, $n = 3-4$ experiments. * $p < 0.05$ compared with WT. The scheme and the table depict the sequence of activation of the explored proteins, with a color code to indicate whether the activated proteins are independent of Kv1.3 expression (brown), dependent of Kv1.3 but not distinguishing between WT and SF (green), or with an absolute requirement for WT Kv1.3 (blue).

To explore whether this location is related to the efficiency of IS formation, we used the edited Jurkat clones stimulated with Raji cells to quantify the number of IS and the intensity of the pLAT signaling at the IS (Figure 8b). Both parameters were significantly decreased in SF and KO clones. Altogether, these data indicate that full activation and effective recruitment of LAT at the IS requires WT Kv1.3 channels.

4 | DISCUSSION

4.1 | Kv1.3 channels of T-cells as targets for new therapies

Due to their demonstrated contribution to T-cell-mediated immune responses, Kv1.3 channels represent promising therapeutic targets in autoimmune disorders. Although Kv1.3 inhibitors did not block IS formation (Beeton et al., 2006), they have been shown to decrease

Ca²⁺-induced pathways in T_{EM} cells of animal models and patients with multiple sclerosis, rheumatoid arthritis, and type I diabetes (Beeton et al., 2006; Lam & Wulff, 2011; Rangaraju et al., 2009), offering an opportunity to ameliorate autoimmune responses. Several nonexcluding mechanisms link the functional expression of Kv1.3 channels to T-cell responses and their relative contribution in pathophysiological situations is unclear. Yet, the design of more precise, mechanistically directed, therapeutic tools would benefit from a better understanding of these processes.

4.2 | Molecular mechanisms linking Kv1.3 channels to T-cell activation

Both Kv1.3 and KCa3.1 contribute to the negative resting V_M needed for Ca²⁺ influx after TCR activation, although kinetic models demonstrated that Kv1.3 dominated the membrane potential of T cells regulating Ca²⁺ influx through CRAC channels (Hou et al., 2014).

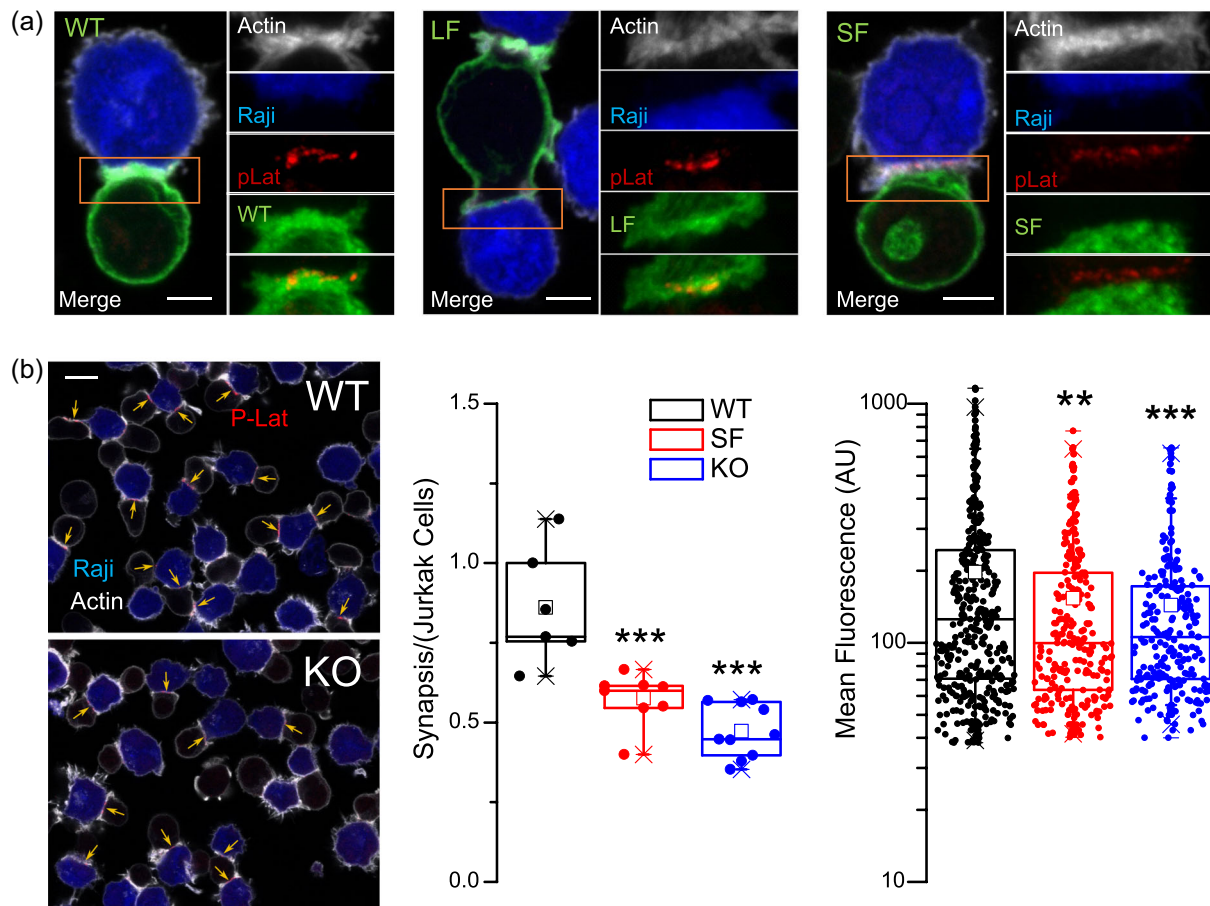


FIGURE 8 Contribution of Kv1.3 channel isoforms to immunological synapse (IS) formation. (a) Representative confocal microscopy images of Jurkat cells transfected with plasmids expressing Kv1.3 isoforms (wild type [WT], long form [LF], or short form [SF]) as enhanced green fluorescent protein (eGFP) fusion proteins (green). Transfected Jurkat cells were exposed to Staphylococcal enterotoxin E (SEE)-loaded Raji B cells and the IS was identified with pLAT staining (red). The actin cytoskeleton was labeled with phalloidin (white) and Raji cells were labeled with CellTracker Blue CMAC dye. Confocal representative images of each condition are shown and the square with the IS is expanded on the right side, to show the four individual channels and the combined green and red (Kv1.3 isoform and pLAT) to evidence the differences in their relative location in each isoform. The expanded images are z-projections of five to eight images around the z plane shown in the corresponding full image. Scale bar = 5 μm . (b) WT, SF, and knockout (KO) Jurkat cells were incubated in the presence of SEE-loaded Raji B cells for 10 min. pLAT, actin, and Raji cells are labeled as indicated and both the number of IS (arrows) normalized to Jurkat cell number and the product of the area and the intensity of the pLAT labeling were quantified in each condition. The plots show the average data from both parameters obtained from triplicates of at least three different experiments per condition. ** $p < 0.01$; *** $p < 0.001$ versus WT. Scale bar = 10 μm .

Besides V_M regulation, Kv1.3-mediated protein–protein interactions modulate the activity of various signaling pathways. Kv1.3 colocalizes with the TCR/CD3 complex in lipid rafts of Jurkat cells and redistributes to the IS formed with APC (Antigen Presenting Cells, Nicolaou et al., 2009; Panyi et al., 2004; Sebestyén et al., 2022). Activity of ion channels at the IS may alter the local ion composition in the restricted volume of the synaptic cleft, modulating the function of voltage-gated channels and other molecules. In addition, Kv1.3 interaction with membrane-associated proteins (such as the adhesion molecule integrin β or actin cytoskeleton), or kinases at the IS has also been reported to participate in signaling to activation in T cells (Artym & Petty, 2002; Chandy et al., 2004; Hajdu et al., 2015; Levite et al., 2000). However, the functional role of these mechanisms (Kv1.3-mediated membrane hyperpolarization vs.

protein–protein interactions) or the role of V_M -dependent changes in these interactions at the IS, is under debate. Although some studies link the immunomodulatory effects of Kv1.3 channels in T cells to their ability to modulate K^+ concentrations, because they were not reproduced with poreless mutant channels (Eil et al., 2016), other reports show that nonconducting Kv1.3 channels could recapitulate WT channel role in the IS formation (Sebestyén et al., 2022).

4.3 | Tools for Kv1.3 channels study and their limitations

Some of these discrepancies arise from the use of overexpression of Kv1.3 WT or mutant channels in T cells that also express endogenous

channels, which may impact the final outcomes. Moreover, the use of Kv1.3 antibodies as the only tool to determine their functional expression has led to confounding results, as most available antibodies lack specificity. Kv channels antibody discovery is limited due to technical challenges. Their membrane topology (multipass regions, multimeric structures), the low immunogenicity of their small surface loops, the high amino acid conservation between family members (leading to immunological tolerance in host animals), and the lack of robust sources of recombinant protein have ranked these proteins among the “high-hanging fruit” in terms of antibody drug discovery (Carter et al., 2017; Wulff et al., 2019).

Here we demonstrate that the use of gene-editing tools to obtain endogenously labeled Kv1.3 channels represents a powerful tool to elucidate channel function, providing unambiguous data on expression and location. We have previously demonstrated that the C-terminal fusion proteins do not alter the expression, the kinetics or the regulation of the Kv1.3 channel protein in heterologous expression systems (Cidad et al., 2012). Here, electrophysiological characterization of edited versus control Jurkat clones did not show changes in current amplitude or kinetics, or in their response to activation (data not shown). Although a potential limitation of this study is the clonal nature of our cells, we minimized its impact by characterizing at least two to three different clones from each construct so that the observed differences could be attributable only to the edited channel (or its absence in the KO).

4.4 | Endogenous Kv1.3 channels express different isoforms

We found endogenous expression of different isoforms of Kv1.3 by alternative translation initiation sites. The mechanisms accounting for the selection of start codons are far from being understood, and cannot be predicted by *in silico* analysis, but there is a small, yet growing, number of mammalian mRNAs that initiate translation from a downstream in-frame AUG (or even a non-AUG codon), producing N-terminal truncated protein isoforms with different functional features (Kochetov, 2008; Touriol et al., 2003). As a mechanism for protein function diversity, alternative translation generates protein isoforms, which, in most cases, are targeted at different subcellular localizations but maintained the same domain contents as the full-length isoforms (Cai et al., 2006). This is consistent with our data showing clearly nonoverlapping locations for LF and SF isoforms. It has also been reported for some other ion channels (Desai et al., 2015; Kisselbach et al., 2014; Touriol et al., 2003). In the case of Kv channels, given the high homology among them, the presence of different isoforms could be a common feature. In fact, using sequence alignment of all Kv1 channels, we found that Kv1.3 M2 methionine (the start codon for the SF) is conserved in Kv1.1, Kv1.2, Kv1.5, and Kv1.10 channels. The existence of a short isoform in these channels awaits experimental confirmation.

4.5 | Intracellular locations of endogenous Kv1.3 channels

In addition to their expression at the plasma membrane, several studies have suggested that Kv1.3 channels also exist in other cell compartments where they are involved in various signaling processes, again by virtue of both conductive properties and/or protein–protein interactions. A few studies locate Kv1.3 channels in a perinuclear location at the cis-Golgi (Zhu et al., 2014) or at the nuclear membrane (Jang et al., 2015) with undefined functions. Many studies have explored the presence and function of Kv1.3 channel in the mitochondria of both cancer cells and T cells. A MgTx- and PAP-1-sensitive K⁺ current contributing to mitochondrial potential, whose inhibition induced apoptosis, has been described in these cells (Szabò et al., 2005, 2008; Varanita et al., 2022). In all cases, a protein of the same molecular weight than canonical Kv1.3 channel was identified. We were unable to detect WT-Kv1.3 channels (or the LF or SF isoforms) at the mitochondria. No MTS could be identified at the N terminus of Kv1.3 (Szabò et al., 2005). However, Kv channels S4 transmembrane helix shows the signature of the canonical MTS (an alternating pattern of hydrophobic and positively charged residues forming an amphipathic helix) and we identified an in-frame AUG codon upstream of this region that was used to create a truncated isoform (mito-Kv1.3). Western blot analysis did not provide evidence for this additional isoform upon endogenous or heterologous processing of the Kv1.3 channel. Moreover, from the colocalization studies overexpressing mito-Kv1.3 we conclude that if this truncated isoform were expressed, it will not be directed to the mitochondria (Supporting Information: Figure I). Further studies, which can benefit from the tools developed here, will be necessary to solve this controversy.

4.6 | Role of Kv1.3 channel isoforms in T-cell activation

Unexpectedly, Jurkat clones expressing only SF or even the KO cells were uncompromised in their ability to perform effector functions such as cytokine secretion. Although at the single-cell level Kv1.3 channel blockers fully abrogate channel function, only partial inhibition with highly variable results of T-cell responses has been detected using functional readouts, such as proliferation or cytokine production, ranging from nonsignificant to >80% block (Beeton et al., 2006; Edwards et al., 2014; Liu et al., 2002; Schmitz et al., 2005). In fact, a recent work using a Kcna3^{-/-} rat has demonstrated that Kv1.3 KO T cells were uncompromised in their ability to perform effector functions. In this case, they found a compensatory upregulation of KCa3.1 that maintained T-cell proliferation and effector responses (Chiang et al., 2017). Moreover, other channel types apart from K⁺ channels (CRAC channels, or certain TRP channels such as TRPV1 or TRPM4) may also have a role in T-cell activation (Bertin et al., 2014; Chen et al., 2013; Launay et al., 2004). These potential compensatory effects were not explored in our

clones. However, the absence of Kv1.3-dependent changes in cytokine secretion led us to study Kv1.3 contribution to intermediate signaling pathways.

TCR signal transduction is initiated by the phosphorylation of TCR and CD3 chains followed by recruitment and phosphorylation of the ZAP70 kinase. These early events at the engaged TCR complex propagated by means of phosphorylation of adaptor molecules, regarded as signaling hubs for TCR signal diversification. LAT and SLP76, the best-characterized adaptor molecules in T cells, exert their functions by mechanisms relying not only on the formation of signalosomes but also on their location within the cell (Jordan et al., 2003; Saveanu et al., 2019). Phosphorylation of membrane-bound LAT activates PLC γ , Ras-MAPK pathway, and SLP76. pSLP76 is recruited to the IS, where it binds integrin VLA-4 ($\alpha 4\beta 1$), stabilizes PLC γ and Ras-MAPK pathways, and regulates other pathways dependent of VLA-4 ligation, including NFAT and nuclear factor- κ B activation, cytokine production, and proliferation (Nguyen et al., 2008). These effectors regulated cytoskeletal morphology, which is profoundly influenced by integrin ligation, so that SLP76 represents an integrator for both TCR and integrins signals.

Similar to SLP76 and LAT molecules, both Kv1.3 channel function as ion pore, and Kv1.3 location and molecular interactions seem to be relevant for T-cell activation at the IS. Accordingly, we found a differential contribution of Kv1.3 channels to the signal transduction steps explored and, more interestingly, a differential contribution of the SF isoforms. Kv1.3 channels are not required for the proximal TCR events (CD3 ζ or ZAP70 phosphorylation are Kv1.3 independent), but they participate in more distal ones, from linkers activation to PLC γ and ERK phosphorylation. Although the intracellular SF isoform retain the function of the WT-Kv1.3 on activation of LAT, ERK, and PLC γ , it cannot supplant the Kv1.3 role on SLP76 recruitment. These results can reflect either the need of an ion conducting channel at the cell membrane for SLP76 activation or the importance of the protein location. We would need to study the effect of a pore dead channel on SLP76 activation to distinguish between these two possibilities. However, Kv1.3 channels have been shown to associate with integrins and cortactin, contributing to actin polymerization (Artym & Petty, 2002; Hajdu et al., 2015; Levite et al., 2000), which harmonizes with the importance of integrin binding for SLP76 translocation and activation.

Although TCR-induced phosphorylation of some key signaling molecules was altered in SF and KO cells, no significant changes in the production of cytokines were observed (Figure 6). The reason could be that the conditions used for production of cytokines are optimal thus masking a partial inhibition. Alternatively, the absence of Kv1.3 channels may affect other functions such as survival or differentiation, which requires further analyses.

Nevertheless, we could confirm that the deficiencies in the TCR signaling pathways in the absence of WT-Kv1.3 led to altered IS formation. In spite of the differences observed on protein phosphorylation between SF and KO clones, we found a significant decrease in the number of conjugates (Jurkat/Raji cell contact) and the intensity of phosphorylated LAT in IS formed in both cases, which is

compatible with a deficient adhesion of T cells to antigen-presenting cells. Changes in both molecular interactions and membrane potential could explain the observed changes.

4.7 | Concluding remarks

We describe here for the first time the endogenous expression of several Kv1.3 channel isoforms in Jurkat cells, showing different location and functional contribution to cell signaling. In particular, the effects on TCR signal transduction of the SF evidence that some of the functions of Kv1.3 channels do not require their presence at the plasma membrane. Altogether, we have developed a powerful tool for exploring regulation of endogenous channels translation and trafficking. On a more general aspect, we demonstrated that, despite being encoding by a single exon, *KCNA3* gene gives rise to several isoforms with different location and function, uncovering a previously overlooked mechanism to increase protein diversity. Given the high homology among Kv1 subfamily members, this could represent a conserved mechanism for other Kv channels.

ACKNOWLEDGMENTS

We thank Esperanza Alonso for excellent technical assistance and Dr Javier Casas (Microscopy Unit, IBGM) for technical support with confocal image analyses. Supported by the Spanish Ministerio de Economía y Competitividad (Mineco, grant PID 2020-118517RB-I00 to M. Teresa Pérez-García and José R. López-López), the Junta de Castilla y León (grants VA172P20 to M. Teresa Pérez-García; Unidad de Excelencia CLU-2019-02 to IBGM, and postdoctoral [DPP] and predoctoral [SME] contracts) and funds from Institut Curie, INSERM, Agence Nationale de la Recherche RetroTact ANR-20CE15-0009-01, ANR-10-IDEX-0001-02 PSL*, and ANR-11-LABX-0043, and Fondation pour la Recherche Médicale FRM EQU202003010280 (Claire Hivroz). Julia Serna and Dino Gobelli are funded by predoctoral contracts of Universidad de Valladolid.

CONFLICT OF INTEREST STATEMENT

The authors declare no conflict of interest.

ORCID

M. Teresa Pérez-García  <http://orcid.org/0000-0001-8540-8117>

REFERENCES

- Artym, V. V., & Petty, H. R. (2002). Molecular proximity of Kv1.3 voltage-gated potassium channels and $\beta 1$ -Integrins on the plasma membrane of melanoma cells. *Journal of General Physiology*, 120(1), 29–37. <http://jgp.rupress.org/content/120/1/29.long>
- Beeton, C., Wulff, H., Standifer, N. E., Azam, P., Mullen, K. M., Pennington, M. W., Kolski-Andreaco, A., Wei, E., Grino, A., Counts, D. R., Wang, P. H., LeeHealey, C. J., S. Andrews, B., Sankaranarayanan, A., Homerick, D., Roeck, W. W., Tehranzadeh, J., Stanhope, K. L., Zimin, P., ... Chandy, K. G. (2006). Kv1.3 channels are a therapeutic target for T cell-mediated autoimmune diseases. *Proceedings of the National Academy of Sciences*, 103(46), 17414–17419. <https://doi.org/10.1073/pnas.0605136103>

- Bertin, S., Aoki-Nonaka, Y., De Jong, P. R., Nohara, L. L., Xu, H., Stanwood, S. R., Srikanth, S., Lee, J., To, K., Abramson, L., Yu, T., Han, T., Touma, R., Li, X., González-Navajas, J. M., Herdman, S., Corr, M., Fu, G., Dong, H., ... Raz, E. (2014). The ion channel TRPV1 regulates the activation and proinflammatory properties of CD4⁺ T cells. *Nature Immunology*, 15(11), 1055–1063. <https://doi.org/10.1038/NI.3009>
- Cahalan, M. D., & Chandy, K. G. (2009). The functional network of ion channels in T lymphocytes. *Immunological Reviews*, 231(1), 59–87. <https://doi.org/10.1111/j.1600-065X.2009.00816.x>
- Cai, J., Huang, Y., Li, F., & Li, Y. (2006). Alteration of protein subcellular location and domain formation by alternative translational initiation. *Proteins: Structure, Function, and Bioinformatics*, 62(3), 793–799. <https://doi.org/10.1002/PROT.20785>
- Carter, P. J., & Lazar, G. A. (2017). Next generation antibody drugs: Pursuit of the “high-hanging fruit”. *Nature Reviews Drug Discovery*, 17(3), 197–223. <https://doi.org/10.1038/nrd.2017.227>
- Chandy, K. G., Wulff, H., Beeton, C., Pennington, M., Gutman, G. A., & Cahalan, M. D. (2004). K⁺ channels as targets for specific immunomodulation. *Trends In Pharmacological Sciences*, 25(5), 280–289. <https://doi.org/10.1016/j.tips.2004.03.010>
- Chen, G., Panicker, S., Lau, K. Y., Apparsundaram, S., Patel, V. A., Chen, S. L., Soto, R., Jung, J. K. C., Ravindran, P., Okuhara, D., Bohnert, G., Che, Q., Rao, P. E., Allard, J. D., Badi, L., Bitter, H. M., Nunn, P. A., Narula, S. K., & DeMartino, J. A. (2013). Characterization of a novel CRAC inhibitor that potently blocks human T cell activation and effector functions. *Molecular Immunology*, 54(3–4), 355–367. <https://doi.org/10.1016/J.MOLIMM.2012.12.011>
- Chiang, E. Y., Li, T., Jeet, S., Peng, I., Zhang, J., Lee, W. P., DeVoss, J., Caplazi, P., Chen, J., Warming, S., Hackos, D. H., Mukund, S., Koth, C. M., & Grogan, J. L. (2017). Potassium channels Kv1.3 and KCa3.1 cooperatively and compensatorily regulate antigen-specific memory T cell functions. *Nature Communications*, 8, 14644. <https://doi.org/10.1038/NCOMMS14644>
- Cidad, P., Alonso, E., Arévalo-Martínez, M., Calvo, E., de la Fuente, M. A., Pérez-García, M. T., & López-López, J. R. (2021). Voltage-dependent conformational changes of Kv1.3 channels activate cell proliferation. *Journal of Cellular Physiology*, 236, 4330–4347. <https://doi.org/10.1002/jcp.30170>
- Cidad, P., Jiménez-Pérez, L., García-Arribas, D., Miguel-Velado, E., Tajada, S., Ruiz-Mcdavitt, C., López-López, J. R., & Pérez-García, M. T. (2012). Kv1.3 channels can modulate cell proliferation during phenotypic switch by an ion-flux independent mechanism. *Arteriosclerosis, Thrombosis, and Vascular Biology*, 32(5), 1299–1307. <https://doi.org/10.1161/ATVBAHA.111.242727>
- Cidad, P., Moreno-Domínguez, A., Novensá, L., Roqué, M., Barquín, L., Heras, M., Pérez-García, M. T., & López-López, R. (2010). Characterization of ion channels involved in the proliferative response of femoral artery smooth muscle cells. *Arteriosclerosis, Thrombosis, and Vascular Biology*, 30(6), 1203–1211. <https://doi.org/10.1161/ATVBAHA.110.205187>
- DeCoursey, T. E., Chandy, K. G., Gupta, S., & Cahalan, M. D. (1984). Voltage-gated K⁺ channels in human T lymphocytes: A role in mitogenesis. *Nature*, 307(5950), 465–468. <https://doi.org/10.1038/307465a0>
- Desai, P. N., Zhang, X., Wu, S., Janoshazi, A., Bolimuntha, S., Putney, J. W., & Trebak, M. (2015). Multiple types of calcium channels arising from alternative translation initiation of the Orai1 message. *Science Signaling*, 8(387). <https://doi.org/10.1126/SCISIGNAL.AAA8323>
- Edwards, W., Fung-Leung, W. P., Huang, C., Chi, E., Wu, N., Liu, Y., Maher, M. P., Bonesteel, R., Connor, J., Fellows, R., Garcia, E., Lee, J., Lu, L., Ngo, K., Scott, B., Zhou, H., Swanson, R. V., & Wickenden, A. D. (2014). Targeting the ion channel Kv1.3 with scorpion venom peptides engineered for potency, selectivity, and half-life. *Journal of Biological Chemistry*, 289(33), 22704–22714. <https://doi.org/10.1074/jbc.M114.568642>
- Eil, R., Vodnala, S. K., Clever, D., Klebanoff, C. A., Sukumar, M., Pan, J. H., Palmer, D. C., Gros, A., Yamamoto, T. N., Patel, S. J., Guittard, G. C., Yu, Z., Carbonaro, V., Okkenhaug, K., Schrupp, D. S., Linehan, W. M., Roychoudhuri, R., & Restifo, N. P. (2016). Ionic immune suppression within the tumour microenvironment limits T cell effector function. *Nature*, 537(7621), 539–543. <https://doi.org/10.1038/nature19364>
- Feske, S., Wulff, H., & Skolnik, E. Y. (2015). Ion channels in innate and adaptive immunity. *Annual Review of Immunology*, 33, 291–353. <https://doi.org/10.1146/annurev-immunol-032414-112212>
- Hajdu, P., Martin, G. V., Chimote, A. A., Szilagy, O., Takimoto, K., & Conforti, L. (2015). The C-terminus SH3-binding domain of Kv1.3 is required for the actin-mediated immobilization of the channel via cortactin. *Molecular Biology of the Cell*, 26(9), 1640–1651. <https://doi.org/10.1091/mbc.E14-07-1195>
- Heijne, G., Steppuhn, J., & Herrmann, R. G. (1989). Domain structure of mitochondrial and chloroplast targeting peptides. *European Journal of Biochemistry*, 180(3), 535–545. <https://doi.org/10.1111/J.1432-1033.1989.TB14679.X>
- Hou, P., Zhang, R., Liu, Y., Feng, J., Wang, W., Wu, Y., & Ding, J. (2014). Physiological role of Kv1.3 channel in T lymphocyte cell investigated quantitatively by kinetic modeling. *PLoS One*, 9(3), e89975. <https://doi.org/10.1371/JOURNAL.PONE.0089975>
- Jang, S. H., Byun, J. K., Jeon, W. I., Choi, S. Y., Park, J., Lee, B. H., Yang, J. E., Park, J. B., O'Grady, S. M., Kim, D. Y., Ryu, P. D., Joo, S. W., & Lee, S. Y. (2015). Nuclear localization and functional characteristics of voltage-gated potassium channel Kv1.3. *Journal of Biological Chemistry*, 290(20), 12547–12557. <https://doi.org/10.1074/jbc.M114.561324>
- Jiménez-Pérez, L., Cidad, P., Álvarez-Miguel, I., Santos-Hipólito, A., Torres-Merino, R., Alonso, E., de la Fuente, M. Á., López-López, J. R., & Pérez-García, M. T. (2016). Molecular determinants of Kv1.3 potassium Channels-Induced proliferation. *The Journal of Biological Chemistry*, 291(7), 3569–3580. <https://doi.org/10.1074/jbc.M115.678995>
- Jordan, M. S., Singer, A. L., & Koretzky, G. A. (2003). Adaptors as central mediators of signal transduction in immune cells. *Nature Immunology*, 4(2), 110–116. <https://doi.org/10.1038/ni0203-110>
- Kisselbach, J., Seyler, C., Schweizer, P. A., Gerstberger, R., Becker, R., Katus, H. A., & Thomas, D. (2014). Modulation of K2P2.1 and K2P10.1 K⁺ channel sensitivity to carvedilol by alternative mRNA translation initiation: ATI regulates drug sensitivity of K2Pchannels. *British Journal of Pharmacology*, 171(23), 5182–5194. <https://doi.org/10.1111/BPH.12596>
- Kochetov, A. V. (2008). Alternative translation start sites and hidden coding potential of eukaryotic mRNAs. *BioEssays*, 30(7), 683–691. <https://doi.org/10.1002/BIES.20771>
- Koni, P. A., Khanna, R., Chang, M. C., Tang, M. D., Kaczmarek, L. K., Schlichter, L. C., & Flavell, R. A. (2003). Compensatory anion currents in Kv1.3 channel-deficient thymocytes. *Journal of Biological Chemistry*, 278(41), 39443–39451. <https://doi.org/10.1074/jbc.M304879200>
- Lam, J., & Wulff, H. (2011). The lymphocyte potassium channels Kv1.3 and KCa3.1 as targets for immunosuppression. *Drug Development Research*, 72(7), 573–584. <https://doi.org/10.1002/ddr.20467>
- Launay, P., Cheng, H., Srivatsan, S., Penner, R., Fleig, A., & Kinet, J.-P. (2004). TRPM4 regulates calcium oscillations after T cell activation. *Science*, 306(5700), 1374–1377. <https://doi.org/10.1126/science.1098845>
- Levite, M., Cahalan, L., Peretz, A., Hershkovitz, R., Sobko, A., Ariel, A., Desai, R., Attali, B., & Lider, O. (2000). Extracellular K⁽⁺⁾ and opening of voltage-gated potassium channels activate T cell integrin function: Physical and functional association between Kv1.3 channels and

- beta1 integrins. *The Journal of Experimental Medicine*, 191(7), 1167–1176. <https://doi.org/10.1084/jem.191.7.1167>
- Lin, C. S., Boltz, R. C., Blake, J. T., Nguyen, M., Talento, A., Fischer, P. A., Springer, M. S., Sigal, N. H., Slaughter, R. S., & Garcia, M. L. (1993). Voltage-gated potassium channels regulate calcium-dependent pathways involved in human T lymphocyte activation. *Journal of Experimental Medicine*, 177(3), 637–645. <https://doi.org/10.1084/JEM.177.3.637>
- Liu, Q. H., Fleischmann, B. K., Hondowicz, B., Maier, C. C., Turka, L. A., Yui, K., Kotlikoff, M. I., Wells, A. D., & Freedman, B. D. (2002). Modulation of Kv channel expression and function by TCR and costimulatory signals during peripheral CD4+ lymphocyte differentiation. *Journal of Experimental Medicine*, 196(7), 897–909. <https://doi.org/10.1084/JEM.20020381>
- Nguyen, K., Sylvain, N. R., & Bunnell, S. C. (2008). T cell costimulation via the integrin VLA-4 inhibits the actin-dependent centralization of signaling microclusters containing the adaptor SLP-76. *Immunity*, 28(6), 810–821. <https://doi.org/10.1016/J.IMMUNI.2008.04.019>
- Nicolaou, S. A., Neumeier, L., Steckly, A., Kucher, V., Takimoto, K., & Conforti, L. (2009). Localization of Kv1.3 channels in the immunological synapse modulates the calcium response to antigen stimulation in T lymphocytes. *Journal of Immunology*, 183(10), 6296–6302. <https://doi.org/10.4049/jimmunol.0900613>
- Panyi, G. (2005). Biophysical and pharmacological aspects of K+ channels in T lymphocytes. *European Biophysics Journal: EBJ*, 34(6), 515–529. <https://doi.org/10.1007/s00249-005-0499-3>
- Panyi, G., Vámosi, G., Bacsó, Z., Bagdány, M., Bodnár, A., Varga, Z., Gáspár, R., Mátyus, L., & Damjanovich, S. (2004). Kv1.3 potassium channels are localized in the immunological synapse formed between cytotoxic and target cells. *Proceedings of the National Academy of Sciences*, 101(5), 1285–1290. <https://doi.org/10.1073/pnas.0307421100>
- Pérez-García, M. T., Ciudad, P., & López-López, J. R. (2018). The secret life of ion channels: Kv1.3 potassium channels and proliferation. *American Journal of Physiology-Cell Physiology*, 314(1), C27–C42. <https://doi.org/10.1152/ajpcell.00136.2017>
- Rangaraju, S., Chi, V., Pennington, M. W., & Chandy, K. G. (2009). Kv1.3 potassium channels as a therapeutic target in multiple sclerosis. *Expert Opinion on Therapeutic Targets*, 13(8), 909–924. <https://doi.org/10.1517/14728220903018957>
- Saez, J., Dogniaux, S., Shafaq-Zadah, M., Johannes, L., Hivroz, C., & Zucchetti, A. (2021). Retrograde and anterograde transport of Lat- vesicles during the immunological synapse formation: Defining the finely-tuned mechanism. *Cells*, 10(2), 359. <https://doi.org/10.3390/CELLS10020359>
- Saveanu, L., Zucchetti, A. E., Evnouchidou, I., Ardouin, L., & Hivroz, C. (2019). Is there a place and role for endocytic TCR signaling. *Immunological Reviews*, 291(1), 57–74. <https://doi.org/10.1111/IMR.12764>
- Schmitz, A., Sankaranarayanan, A., Azam, P., Schmidt-Lassen, K., Homerick, D., Hänsel, W., & Wulff, H. (2005). Design of PAP-1, a selective small molecule Kv1.3 blocker, for the suppression of effector memory T cells in autoimmune diseases. *Molecular Pharmacology*, 68(5), 1254–1270. <https://doi.org/10.1124/mol.105.015669.nally>
- Sebestyén, V., Nagy, É., Mocsár, G., Volkó, J., Szilágyi, O., Kenesei, Á., Panyi, G., Tóth, K., Hajdu, P., & Vámosi, G. (2022). Role of C-Terminal domain and membrane potential in the mobility of Kv1.3 channels in immune synapse forming T cells. *International Journal of Molecular Sciences*, 23(6), 3313. <https://doi.org/10.3390/IJMS23063313/S1>
- Szabó, I., Bock, J., Grassmé, H., Soddemann, M., Wilker, B., Lang, F., Zoratti, M., & Gulbins, E. (2008). Mitochondrial potassium channel Kv1.3 mediates Bax-induced apoptosis in lymphocytes. *Proceedings of the National Academy of Sciences*, 105(39), 14861–14866. <https://doi.org/10.1073/pnas.0804236105>
- Szabó, I., Bock, J., Jekle, A., Soddemann, M., Adams, C., Lang, F., Zoratti, M., & Gulbins, E. (2005). A novel potassium channel in lymphocyte mitochondria. *Journal of Biological Chemistry*, 280(13), 12790–12798. <https://doi.org/10.1074/jbc.M413548200>
- Touriol, C., Bornes, S., Bonnal, S., Audigier, S., Prats, H., Prats, A. C., & Vagner, S. (2003). Generation of protein isoform diversity by alternative initiation of translation at non-AUG codons. *Biology of the Cell*, 95(3–4), 169–178. [https://doi.org/10.1016/S0248-4900\(03\)00033-9](https://doi.org/10.1016/S0248-4900(03)00033-9)
- Urrego, D., Tomczak, A. P., Zahed, F., Stühmer, W., & Pardo, L. A. (2014). Potassium channels in cell cycle and cell proliferation. *Philosophical Transactions of the Royal Society, B: Biological Sciences*, 369(1638), 20130094. <https://doi.org/10.1098/rstb.2013.0094>
- Varanita, T., Angi, B., Scattolini, V., & Szabo, I. (2023). Kv1.3 K + channel physiology assessed by genetic and pharmacological modulation. *Physiology (Bethesda, Md.)*, 38(1), 25–41. <https://doi.org/10.1152/PHYSIOL.00010.2022>
- Wulff, H., Calabresi, P. A., Allie, R., Yun, S., Pennington, M., Beeton, C., & Chandy, K. G. (2003). The voltage-gated Kv1.3 K + channel in effector memory T cells as new target for MS. *Journal of Clinical Investigation*, 111(11), 1703–1713. <https://doi.org/10.1172/JCI200316921.Introduction>
- Wulff, H., Castle, N. A., & Pardo, L. A. (2009). Voltage-gated potassium channels as therapeutic targets. *Nature Reviews Drug Discovery*, 8(12), 982–1001. <https://doi.org/10.1038/nrd2983>
- Wulff, H., Christophersen, P., Colussi, P., Chandy, K. G., & Yarov-Yarovoy, V. (2019). Antibodies and venom peptides: New modalities for ion channels. *Nature Reviews Drug Discovery*, 18, 339–357. <https://doi.org/10.1038/s41573-019-0013-8>
- Zhao, N., Dong, Q., Du, L. L., Fu, X. X., Du, Y. M., & Liao, Y. H. (2013). Potent suppression of Kv1.3 potassium channel and IL-2 secretion by diphenyl phosphine oxide-1 in human T cells. *PLoS One*, 8(5), e64629. <https://doi.org/10.1371/JOURNAL.PONE.0064629>
- Zhu, J., Yan, J., & Thornhill, W. B. (2014). The Kv1.3 potassium channel is localized to the cis-Golgi and Kv1.6 is localized to the endoplasmic reticulum in rat astrocytes. *FEBS Journal*, 281(15), 3433–3445. <https://doi.org/10.1111/febs.12871>

SUPPORTING INFORMATION

Additional supporting information can be found online in the Supporting Information section at the end of this article.

How to cite this article: Serna, J., Peraza, D. A., Moreno-Estar, S., Saez, J. J., Gobelli, D., Simarro, M., Hivroz, C., López-López, J. R., Ciudad, P., Fuente, M. A. d. I., & Pérez-García, M. T. (2023). Characterization of endogenous Kv1.3 channel isoforms in T cells. *Journal of Cellular Physiology*, 1–16. <https://doi.org/10.1002/jcp.30984>